Effect of quantized electronic states on the dispersive Raman features in individual single-wall carbon nanotubes

A. G. Souza Filho,[1,2] A. Jorio,[1] G. Dresselhaus,[3] M. S. Dresselhaus,[1,4] R. Saito,[5] A. K. Swan,[6] M. S. Ünlü,[6] B. B. Goldberg,[6,7] J. H. Hafner,[8] C. M. Lieber,[8] and M. A. Pimenta[9]

[1]*Department of Physics, Massachusetts Institute of Technology, Cambridge, Massachusetts 02139-4307*
[2]*Departamento de Física, Universidade Federal do Ceará, Fortaleza-CE, 60455-760, Brazil*
[3]*Francis Bitter Magnet Laboratory, Massachusetts Institute of Technology, Cambridge, Massachusetts 02139*
[4]*Department of Electrical Engineering and Computer Science, Massachusetts Institute of Technology, Cambridge, Massachusetts 02139-4307*
[5]*Department of Electronic-Engineering, University of Electro-Communications, Tokyo, 182-8585, Japan*
[6]*Electrical and Computer Engineering Department, Boston University, Boston, Massachusetts 02215*
[7]*Department of Physics, Boston University, Boston, Massachusetts 02215*
[8]*Department of Chemistry, Harvard University, Cambridge, Massachusetts 02138*
[9]*Departamento de Física, Universidade Federal de Minas Gerais, Belo Horizonte - MG, 30123-970, Brazil*

(Received 28 August 2001; published 19 December 2001)

This work reports how resonance Raman experiments are used to study details of the electronic structure of individual single-wall carbon nanotubes (SWNTs) by measuring the phonon spectra and how the quantized electronic structure affects the dispersive Raman features of SWNTs. We focus our analysis on the dispersive D and G' bands observed in the Raman spectra of isolated semiconducting nanotubes. By using a laser excitation energy of 2.41 eV, we show that both the D-band and G'-band frequencies are dependent on the wave vector k_{ii} where the electrons are confined in the one-dimensional subband i of the electronic structure of SWNTs. By making use of the (n,m) assignment for each tube, we theoretically correlate the observed frequency dependences for the D- and G'-band modes with the electronic structure predicted for each (n,m) pair and we determine the dependence of ω_D and $\omega_{G'}$ on the diameter and chirality for individual electronic transitions E_{ii} for nanotube bundles. We use the D- and G'-band dependence on electron wave vector k_{ii} to predict the dominant phonon wave vector q selected by the quantum-confined electronic state k_{ii} and to explain the anomalous dispersion observed for ω_D and $\omega_{G'}$ in SWNT bundles as a function of laser excitation energy, yielding excellent agreement between experiment and theory.

DOI: 10.1103/PhysRevB.65.035404 PACS number(s): 78.30.Na, 78.30.−j

I. INTRODUCTION

The disorder-induced D band that appears in the Raman spectra of sp^2 carbon materials was first observed in 1970.[1] This band is only activated in the Raman spectrum in sp^2 carbons in the presence of heteroatoms, vacancies, grain boundaries, or any defect that lowers the crystal symmetry of the quasi-infinite lattice, thus relaxing the $q\sim 0$ zone-center selection rule for first-order Raman scattering. The most interesting characteristic of the disorder-induced D band and of its second-order related G'-band feature in the Raman spectra of sp^2-bonded carbon materials is their strongly dispersive behavior as a function of laser excitation energy E_{laser}. The G' band is indeed an intrinsic feature of sp^2 carbons, which is always observed in the Raman spectra, even when the D band is absent.[2]

The E_{laser} dependence of the ω_D and $\omega_{G'}$ bands has been interpreted as due to a k-selective resonance process that occurs between the linearly dispersive π and π^* electronic states.[2–4] The physical origin of this k selection condition was explained by a double-resonance process which involves a resonance not only with the incident or scattered photons, but also with an intermediate intraband scattering process.[5] The phonons that contribute to the D-band and G'-band features come from the boundary region of the graphite Brillouin zone (K point). The D-band and G'-band features are also observed in the Raman spectra of single-wall nanotube bundles[6–8] and more recently in isolated single-walled carbon nanotubes (SWNTs).[9]

Of special interest in the study of the dispersive D and G' bands is the information about the electronic structure of SWNTs that is conveyed by their phonon spectra. To explain how the details of the electronic structure of SWNTs can be probed by the phonon spectra and to determine how the quantized electronic states affect the dispersive D-band and G'-band features in the SWNT Raman spectra are the goals of the present paper. We thus present here a study of the disorder-induced D-band frequency and its overtone G'-band frequency in isolated SWNTs by correlating the phonon properties with the calculated electronic structure implied by the (n,m) indices. An earlier study of the D band for isolated tubes[9] reported that the D band is observed only for nanotubes for which the laser energy is in resonance with interband transitions between van Hove singularities in the one-dimensional (1D) density of electronic states.[9] To gain a more precise understanding of the D-band properties of isolated SWNTs, as compared to earlier studies on an ensemble of isolated SWNTs,[9] the present experiments were carried out using a very dilute nanotube density sample to ensure that all the features in the Raman spectrum come from one

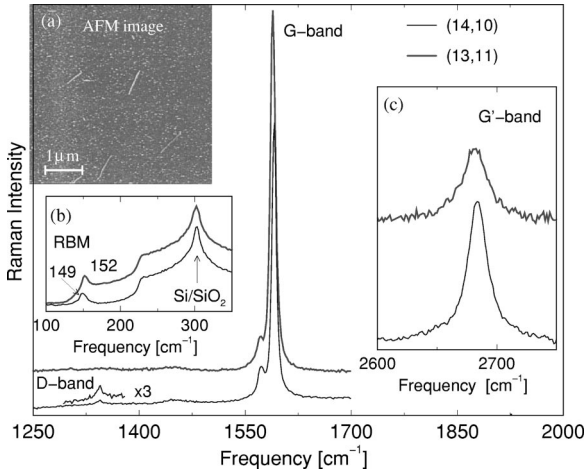

FIG. 1. Two typical Raman *D*-band and *G*-band spectra obtained from single isolated SWNTs using $E_{\text{laser}}=2.41$ eV. The upper and lower spectra are for the (14,10) and (13,11) nanotubes, respectively. Inset (a) shows an atomic force microscope (AFM) image of the isolated nanotubes on a Si/SiO_2 substrate used in this study, where only four tubes are observed in a 25 μm^2 area. Inset (b) shows the spectra for each tube in the frequency range of the radial breathing mode which is used for obtaining the (n,m) identification of these tubes. The Raman frequencies are displayed in units of cm^{-1}. Inset (c) shows the Raman spectra in the region of the G' band for the (14,10) and (13,11) nanotubes.

and the same resonant SWNT. In this way, the (n,m) indices can be determined from an analysis of the radial breathing mode (RBM) feature for the nanotubes under investigation for their *D*-band and G'-band characteristics. This procedure allowed a detailed study at fixed E_{laser} to be carried out of the ω_D and $\omega_{G'}$ dependence on the (n,m) indices. Based on the physical origin of the *D* and G' bands, whereby a double-resonance process selects the dominant phonon wave vectors, our results show how the electrons and phonons are strongly coupled under resonant conditions, thus revealing that the van Hove singularities play the dominant role in determining both the *D*-band and G'-band intensity and frequency in isolated SWNTs. By using this property, we reproduce the anomalous dispersion observed in the E_{laser} dependence of ω_D and $\omega_{G'}$ in SWNT bundles.[6,8,10]

II. EXPERIMENT

The upper inset to Fig. 1 shows an atomic force microscope (AFM) image of the isolated SWNT sample used in this work, where in a 25 μm^2 area we can observe only four isolated nanotubes ($\leqslant 1$ SWNT/μm^2), each SWNT with ~ 1.0 μm in length. The AFM image of the whole sample shows a homogeneous spacial distribution of SWNTs with diameters d_t varying from 1.0 to 3.0 nm. The details of the sample preparation are reported elsewhere.[11] Raman spectra from each isolated SWNT were obtained by scanning the sample in steps of 0.5 μm under a controlled microscope stage. The spectral excitation was provided by an Ar ion laser, using the 514.5 nm laser line ($E_{\text{laser}}=2.41$ eV) and with a power density of ~ 1 MW/cm^2 on the sample surface. The scattered light was analyzed with a Renishaw spectrometer 1000B, equipped with a cooled charge-coupled device (CCD) detector.

III. RESULTS AND DISCUSSION

The observation of Raman spectra from just one nanotube is possible because of the very large density of electronic states close to the van Hove singularities of the 1D SWNT electronic structure.[12] When the incident or scattered photons are in resonance with an electronic transition E_{ii} between van Hove singularities in the valence and conduction bands, the Raman cross section becomes very large due to the strong coupling which occurs between the electrons and phonons of the nanotube under these resonance conditions. When the resonance involves a scattered photon, only the phonon that is involved in such a process will be enhanced in the experimentally observed Raman spectrum. However, when the *incident* photon is resonant, *all* the phonons in the Raman spectra are enhanced through the electron excitation process by the E_{laser} photons. In this work we only discuss isolated SWNTs resonant with the incident photon, because it is essential for the radial breathing mode to be resonantly enhanced, so that it can be used to make the (n,m) assignment for the SWNTs that are investigated for their *D*-band and G'-band characteristics. Once (n,m) is identified, we can theoretically calculate the electronic structure for the nanotube under investigation.

Figure 1 shows the Raman spectra (including the RBM, the *D* band, the *G* band, and the G' band) for two isolated SWNTs, with nanotube indices identified as (14,10) and (13,11), using a previously reported method, based on the properties of the RBM under resonance Raman conditions for isolated SWNTs.[12] The *G*-band profiles for both SWNT spectra in Fig. 1 are typical of semiconducting tubes,[13–15] and for both spectra, the splitting of the two most intense components is the same (21 cm^{-1}). This is expected, since both tubes have almost the same diameter as implied by their observed RBM frequencies.[16,17] For the isolated SWNTs studied in this work, the *D*-band intensity is either low compared to that of the *G* band, as in the lower spectrum in Fig. 1, or completely absent (see upper spectrum in Fig. 1), indicating that the isolated SWNTs are highly ordered and contain few defects in their 1D crystalline lattice. However, for all semiconducting tubes measured in this work, the G' band is always observed with frequencies of about $2\omega_D$, and the G'-band feature is always intense, thus confirming that the G' band is independent of whether the nanotube lattice has defects or not.

Once the (n,m) indices are appropriately identified for each isolated tube, we can now study the *D*-band and G'-band frequencies as a function of their (n,m) indices, which means study of ω_D and $\omega_{G'}$ as a function of diameter d_t and chiral angle θ. The assigned tubes in the present paper that are resonant with E_{44}^S in order of increasing reciprocal diameter $1/d_t$ are: (19,6) [$d_t=1.79$ nm, $\theta=13.3°$], (13,12) [$d_t=1.72$ nm, $\theta=28.7°$], (17,7) [$d_t=1.70$ nm, $\theta=16.5°$], (14,10) [$d_t=1.66$ nm, $\theta=24.5°$], (13,11) [$d_t=1.65$ nm, $\theta=27.2°$], (17,6) [$d_t=1.64$ nm, $\theta=14.6°$], (18,4) [d_t

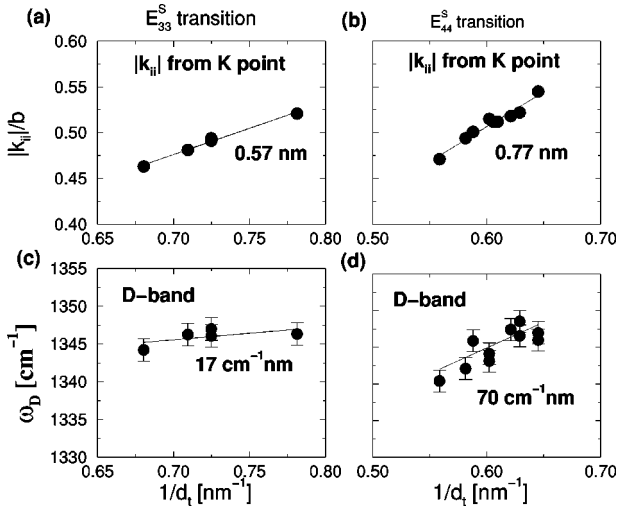

FIG. 2. Distance $|k_{ii}|/b$ to the K point plotted as a function of the reciprocal nanotube diameter for electrons in the 2D Brillouin zone of graphite associated with the (a) E_{33}^S and (b) E_{44}^S electronic transitions between van Hove singularities. b is the magnitude of the basis vectors in the 2D reciprocal graphene lattice. D-band frequencies as a function of reciprocal diameter for individual SWNTs, for which the (c) E_{33}^S and (d) E_{44}^S interband transitions are in resonance with $E_{\text{laser}}=2.41$ eV. The numbers in (a), (b), (c), and (d) denote the slopes of the linear trends represented by the solid lines.

$=1.61$ nm, $\theta=9.8°$], (19,2) [$d_t=1.59$ nm, $\theta=4.9°$], and (15,7) [$d_t=1.55$ nm, $\theta=18.1°$]. The tubes resonant with E_{33}^S in order of increasing reciprocal diameter $1/d_t$ are: (18,1) [$d_t=1.47$ nm, $\theta=2.7°$], (14,6) [$d_t=1.41$ nm, $\theta=17.0°$], (15,2) [$d_t=1.28$ nm, $\theta=6.2°$], (15,4) [$d_t=1.38$ nm, $\theta=11.5°$], and (11,9) [$d_t=1.38$ nm, $\theta=26.7°$].[18]

Figures 2(c) and 2(d) show a plot of the observed D-band frequency ω_{D} (solid circles) vs $1/d_t$ for isolated semiconducting SWNTs resonant with $E_{\text{laser}}=2.41$ eV. Although these data do not show a definitive pattern, we can see that ω_D for isolated SWNTs with 2.41 eV laser excitation have values lower than for 2D graphite at the same E_{laser} excitation for which $\omega_D=1355$ cm^{-1}.[19] Noteworthy is the fact that at the single-nanotube level for the same laser excitation energy, different SWNTs exhibit different ω_D, in contrast to observations on other sp^2 carbon materials where the frequency ω_D is uniquely determined by E_{laser}. The diameter d_t dependences of ω_D in Figs. 2(c) and 2(d) appear to be complex, not being simply related to the diameter dependence of the spring constants, as occurs for the radial breathing mode.[20] As we will discuss below, the spread in the data points shown in Fig. 2 is related to the dependence of ω_D on the nanotube electronic structure.

In graphite and other sp^2 carbons, the D-band frequency is dispersive and the origin of this dispersive behavior was explained on the basis of a double resonance effect.[5] Thus the possible phonon wave vectors q that satisfy the double-resonance conditions can vary from 0 to $2|k|$, where k is the wave vector for the resonantly excited electronic states measured from the K point. In sp^2 carbons in general, the D-band frequency will be mainly determined by the q vectors which satisfy $q\approx 2|k|$.[5,21,22] In the case of SWNTs, the situation is different from sp^2 materials since to observe the D-band spectra experimentally, it is necessary for a resonance to occur with the 1D van Hove singularities in the joint density of states (JDOS) which yields an additional divergence beyond the double-resonance terms given in the Raman intensity formula described in Ref. 5. Then, the van Hove singularity for the electronic states E_{ii} will strongly constrain the k vector involved in the double resonance process, and because of the relation between the electron and phonon wave vectors under double resonance conditions, this constraint will affect the selection of q vectors involved in the double resonance process responsible for the D-band frequency.

The special 1D electronic structure of each nanotube is uniquely determined by its diameter and chirality.[20] In Fig. 3 we plot the equi-energy contours of 2D graphite around the K point in the Brillouin zone considering the linear k approximation for $E(k)$, where both the valence and conduction bands for the π and π^* states are, respectively, symmetric.[20] By using zone folding arguments,[20] the 1D Brillouin zone for nanotubes is given by a set of cutting lines, which are shown in Fig. 3(a) for two specially selected tubes [(13,12) and (13,11)] with similar chiralities and different diameters. In Fig. 3(b) we also show two specially selected tubes [(19,2) and (14,9)] with different chiralities but similar diameters. The one-dimensional van Hove singularities of each SWNT come from the flat regions (both the maxima and minima) in the dispersion relations along the cutting lines in Fig. 3. The positions of the extremal points in the E_{44}^S transition, resonant with $E_{\text{laser}}=2.41$ eV for these particular SWNTs [or the singularities in the JDOS (Ref. 23)], are each indicated by small solid circles and squares in Fig. 3. We define the distance from the K point where the extrema of the E_{ii} energies occur (the van Hove singularities) as $|k_{ii}|$, which is thus seen to depend on nanotube diameter [Fig. 3(a)] as $\propto 1/d_t$, and on the chiral angle θ [Fig. 3(b)] due to the trigonal warping effect.[24]

In Figs. 2(a) and 2(b) we plot the $|k_{ii}|$ for several (n,m) SWNTs that we observed to be in resonance with E_{33}^S and E_{44}^S, respectively. By comparing Fig. 2(a) with 2(c) and Fig. 2(b) with 2(d), the agreement between the trends in ω_D and $|k_{ii}|$ as a function of $1/d_t$ is found to be good for both the E_{44}^S and E_{33}^S transitions, in the sense that the magnitude of the slopes in the $|k_{ii}|$ vs $1/d_t$ plots [Figs. 2(a) and 2(b)] is reflected in the slopes of the ω_D vs $1/d_t$ plots [Figs. 2(c)–2(d)]. The relation between the D-band frequency ω_D and k_{ii} is clearly evident when plotting the results in terms of the chiral angle dependence θ. By considering SWNTs with similar diameters, as in the case of those SWNTs that are in resonance with one of the E_{44}^S or E_{33}^S electronic transitions, we can analyze the D-band frequencies as a function of the chiral angle θ determined by the (n,m) assignment. We then plot the resulting ω_D (solid circles) vs chiral angle (θ) for the SWNTs for which $E_{\text{laser}}=2.41$ eV is resonant with the E_{33}^S [Fig. 4(a)] and with the E_{44}^S [Fig. 4(b)] electronic transitions. This difference in behavior is related to different van Hove singularities, as discussed below.

We then plot the distance $|k_{ii}|$ of the van Hove singulari-

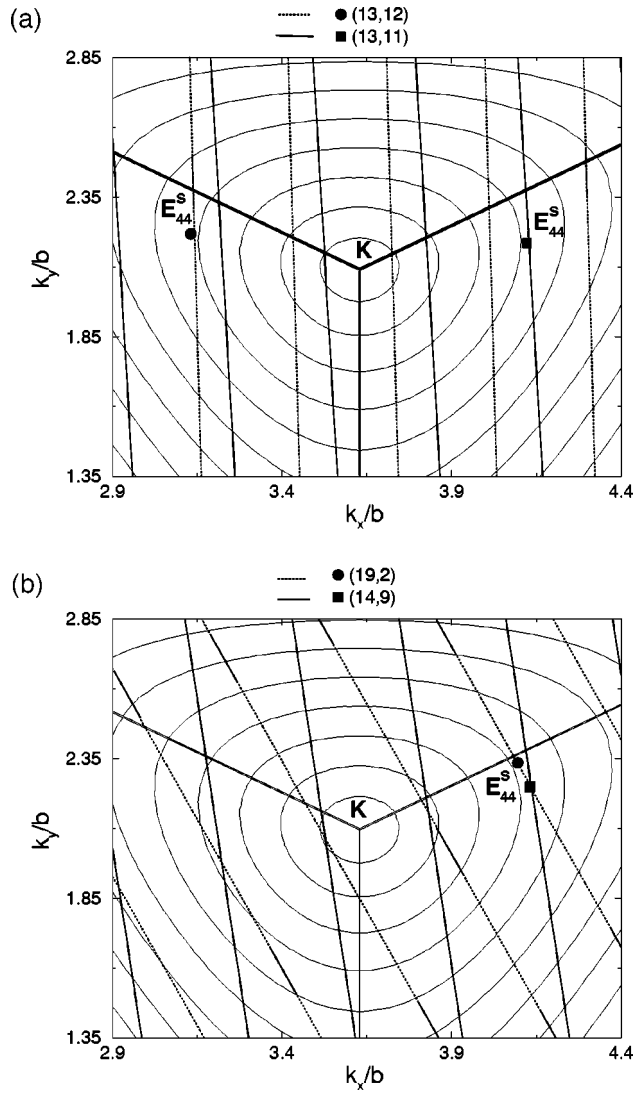

FIG. 3. Equi-energy contours of 2D graphite calculated by the tight-binding method around the K point in the 2D graphene Brillouin zone. The lines are the 1D Brillouin zone of the nanotube. The positions of the van Hove singularities E_{44}^S are shown (a) for the (13,12) (solid circle) and (13,11) (solid square) semiconducting tube with similar chiralities and different diameters and (b) for the (19,2) (solid circle) and (14,9) (solid square) semiconducting tubes with different chiralities and similar diameters. What determines the frequency of the D band and G' band is the distance $|k_{ii}|$ of these singularities from the K point. b is the magnitude of the basis vectors in the 2D graphene reciprocal lattice. The explicit $|k_{ii}|/b$ values are 0.512, 0.494, 0.522, and 0.530 for the (13,11), (13,12), (19,2), and (14,9) nanotubes, respectively.

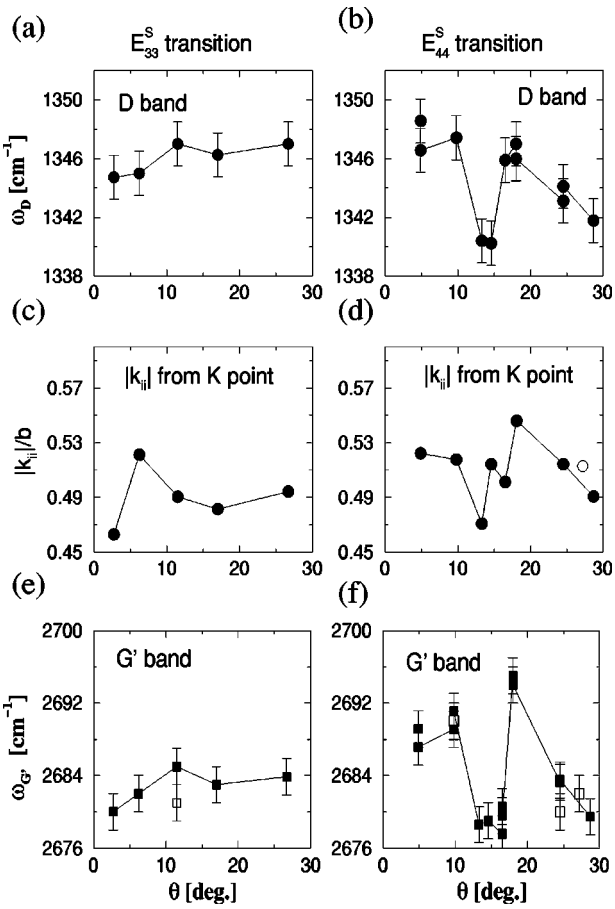

FIG. 4. Measured D-band frequencies as a function of chiral angle θ of SWNTs for which $E_{\text{laser}}=2.41$ eV is in resonance with the E_{33}^S (a) and E_{44}^S (b) interband transitions in the JDOS. The distance $|k_{ii}|/b$ to the K point for electrons in the 2D Brillouin zone of graphite, associated with the E_{ii} van Hove singularities, are plotted vs θ for E_{33} (c) and E_{44} (d) for the tubes measured in (a) and (b). (e) and (f) correspond to (a) and (b) except that the data are for the G' band. The solid and open squares in (e) and (f), respectively, denote $\omega_{G'}$ data for tubes where the D band is (solid points) or is not (open points) observed in the Raman spectrum (see text).

ties in the 2D graphite Brillouin zone from the K point for the observed tubes in our experiments where the E_{33}^S [Fig. 4(c)] and E_{44}^S [Fig. 4(d)] electronic transitions can be in resonance with $E_{\text{laser}}=2.41$ eV. The good agreement between Figs. 4(a) and 4(c) and between Figs. 4(b) and 4(d) shows that ω_D in SWNTs can be explained in terms of the relation between $|k_{ii}|$ for the electrons and q for the phonons, which are resonantly coupled to each other by the double-resonance process.[5] By this agreement, we establish that, in the case of SWNTs, the double resonance is restricted to the k_{ii} states corresponding to the van Hove singularities.

To confirm the chirality dependence of ω_D, we analyze the experimental θ dependence of the G'-band frequency ($\omega_{G'}\approx 2\omega_{\text{D}}$) for the E_{33}^S and E_{44}^S transitions, as shown in Figs. 4(e) and 4(f). A similar θ dependence is seen in Figs. 4(e) and 4(f) for the G' band, as is found in Figs. 4(a) and 4(b) for the D band for both the E_{33}^S and E_{44}^S transitions. This result suggests also plotting in Figs. 4(e) and 4(f) the data for $\omega_{G'}$ vs θ for those Raman spectra where we have identified (n,m) values, but have no D-band intensity. The resulting four additional G'-band data points shown as open squares in Figs. 4(e) and 4(f) also are consistent with the solid data points. Since the observation of the G'-band feature is not limited to the presence of structural defects in the nanotube lattice, and since the E_{laser} is fixed in the present experiment, we confirm that the diameter and chirality effect on ω_D and $\omega_{G'}$ that we observe in Fig. 4 is intrinsically related to the

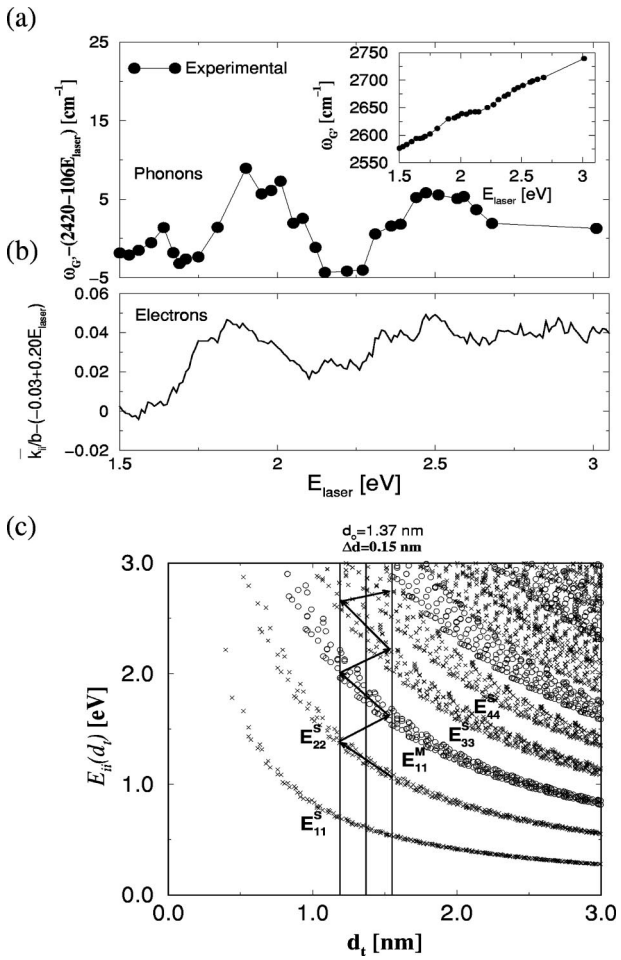

FIG. 5. (a) G'-band data for $\omega_{G'}$ for a SWNT bundle sample taken from Ref. 6 after subtracting the linear dispersion $2420+106E_{\text{laser}}$ from the $\omega_{G'}$ vs E_{laser} data shown in the inset. (b) Calculated first moment $\bar{k}_{ii}/b$ for the possible resonant tubes as a function of E_{laser} after subtracting the linear dispersion $-0.03+0.20E_{\text{laser}}$ (see text). (c) The transition energies E_{ii} between van Hove singularities as a function of diameter (Ref. 24). The vertical lines denote the diameter range of the SWNT bundle used in the G'-band dispersion experiments taken from Ref. 6 [see inset in (a)].

resonant coupling between the phonons and electrons. Therefore, we have shown that the resonance with van Hove singularities E_{ii} plays the dominant role in determining the intensity and frequency of the D band and G' band in individual SWNTs.

By using this unique electron-phonon coupling effect, we show below that we can now explain the physical origin of the anomalous dispersion observed in the $\omega_{G'}$ vs E_{laser} data in SWNT bundles as shown in the inset to Fig. 5(a).[6,8,10] The fit of the experimental data for the G' band for a particular SWNT bundle leads to a linear dispersion $\overline{\omega}_{G'}=2420+106E_{\text{laser}}$ which is superimposed on an oscillation that arises from the different subbands of the SWNTs that are excited with different laser energies, as shown in the inset to Fig. 5(a).[6] The experimental data of Ref. 6 are then plotted in Fig. 5(a) after subtracting the linear dependence that is characteristic of sp^2 carbons. The resulting data points in Fig. 5(a) show a clear oscillatory behavior of $\omega_{G'}$ as a function of E_{laser}. To predict the G'-band dispersion for a particular SWNT sample and to compare the predictions with the experimental results, we proceed as follows. First, we consider the diameter distribution of the SWNT bundle sample that was measured by transmission electron microscopy (TEM) measurements.[13] For this particular SWNT bundle sample, the diameter distribution is represented by the vertical lines (average diameter $d_0=1.37$ nm and deviation $\Delta d=0.18$ nm) in Fig. 5(c), and we assume that only the (n,m) nanotubes in this range of d_t contribute to the Raman spectra. For each E_{laser} value a different set of (n,m) tubes will be within the resonant window, including the incident and scattered photons associated with E_{laser}.[12] The resonant window for the incident photon is given by $E_{\text{laser}}-0.1$ eV $\leq E_{ii} \leq E_{\text{laser}}+0.1$ eV,[12] while scattered photons in the range $E_{\text{laser}}-E_{G'}-0.1$ eV$\leq E_{ii} \leq E_{\text{laser}}-E_{G'}+0.1$ eV will contribute resonantly to the spectra at a lower energy for the Stokes process. The energy of the van Hove singularities E_{ii} and their corresponding k_{ii} values depend on the tight-binding parameter γ_0.[20] For isolated SWNTs, $\gamma_0=2.89$ eV accounts for the observed Raman spectra, but for SWNT bundles, it is expected that there will be some deviation from this value due to the effect of the van der Waals interaction between the tubes in the bundles.[25] Recently, Rao *et al.*[25] reported that this interaction is responsible for an upshift of 0.2 eV in the E_{ii} energy transitions. We, however, find that the data indicate that this shift in the joint density of states can be taken into account, by using $\gamma_0=2.95$ eV, which agrees with the value of $\gamma_0=2.95$ eV obtained by Pimenta *et al.*[13] by fitting the resonant window for metallic tubes and using the same physical sample as was used to measure the G' band shown in Fig. 5(a). For each (n,m) in the resonant window of Ref. 13, we calculated the k_{ii}, and then for each k_{ii} we obtained the first moment $\bar{k}_{ii}$ by weighting each (n,m) diameter by the Gaussian distribution of the nanotubes in the sample. The resulting average of these k_{ii} values was also found to be linear in E_{laser}, but with a superimposed oscillation associated with each E_{ii} branch. After subtracting the linear dispersion $\bar{k}_{ii}=-0.03+0.20E_{\text{laser}}$, we plot $\bar{k}_{ii}$ as a function of E_{laser} in Fig. 5(b), and we find that $\bar{k}_{ii}$ has a behavior that is exactly the same as is observed in the G'-band dispersion [see Fig. 5(a)]. We therefore can conclude that the oscillations in Figs. 5(a) and 5(b) come from the oscillation in $\bar{k}_{ii}$ along each subband, as indicated by the arrows in Fig. 5(c). The analysis presented above clearly demonstrates that the properties of the dispersive D band and G' band in SWNTs have some commonality with graphite in general, but the details can only be described if the 1D electronic structure is considered in detail. We further conclude that the confined electronic states in the flat regions of the electronic dispersion $E(k)$, denoted by the k_{ii} states for each E_{ii} singularity, play the dominant role in observing the D-band and G'-band features in the first place and in determining the values of their frequencies.

IV. CONCLUSION

We have reported a detailed study of the characteristics of the D band and G' band for isolated SWNTs, including their

dependence on the electronic structure that is determined by their (n,m) indices. In contrast to all other sp^2 carbon-based materials, the D and G' bands in isolated SWNTs show a range of different frequencies ω_D and $\omega_{G'}$ for the same laser excitation energy, E_{laser}. The frequency dependence on E_{ii} observed for $\omega_D(\theta)$ and $\omega_{G'}(\theta)$ is a new effect, not yet reported for other phonons observed in the Raman spectrum of isolated SWNTs, where ω_{RBM} and ω_G for semiconducting SWNTs depends only on d_t and not on θ.[20,26] In fact, the observed frequencies arise from the resonant process itself, where the van Hove singularities select the initial electronic states k_{ii} within the 1D Brillouin zone that are responsible for the selection of the phonon q vectors, thus giving different D-band frequencies for different (n,m) values. Our interpretation of the dependence of ω_D and $\omega_{G'}$ on d_t and θ is then confirmed by the excellent agreement between the predicted and observed anomalous E_{laser}-dependent dispersion studies of $\omega_{G'}$ in SWNT bundles.[6] We thus conclude that the resonance with the van Hove singularities in the joint density of states plays the dominant role in determining the frequency of the D band and G' band in isolated SWNTs. The large dispersion of $\omega_{G'}$ gives rise a shift in the G'-band frequency that is sufficiently large to allow one to use phonons to study physical phenomena related to the electronic structure of SWNTs in some detail by the use of resonance Raman spectroscopy measurements at the single nanotube level.

ACKNOWLEDGMENTS

A.G.S.F. and A.J. acknowledge financial support from the Brazilian agencies CAPES and CNPq, respectively. A.K.S., M.S.U., and B.B.G. acknowledge support from Renishaw Inc. The experimental work was performed at Boston University at the Photonics Center, operated in conjunction with the Department of Physics and the Department of Electrical and Computer Engineering. R.S. acknowledges a Grant-in-Aid (No. 13440091) from the Ministry of Education, Japan. The MIT authors acknowledge support under NSF Grant Nos. DMR 01-16042, INT 98-15744, and INT 00-00408.

[1] F. Tuinstra and J.L. Koenig, J. Chem. Phys. **53**, 1126 (1970).
[2] M.J. Matthews, M.A. Pimenta, G. Dresselhaus, M.S. Dresselhaus, and M. Endo, Phys. Rev. B **59**, R6585 (1999).
[3] I. Pócsik, M. Hundhausen, M. Koós, and L. Ley, J. Non-Cryst. Solids **227-230**, 1083 (1998).
[4] A.C. Ferrari and J. Robertson, Phys. Rev. B **61**, 14 095 (2000).
[5] A.V. Baranov, A.N. Bekhterev, Y.S. Bobovich, and V.I. Petrov, Opt. Spectrosk. **62**, 1036 (1987) [Opt. Spectrosc. **62**, 612 (1987)]; C. Thomsen and S. Reich, Phys. Rev. Lett. **85**, 5214 (2000).
[6] M.A. Pimenta, E.B. Hanlon, A. Marucci, P. Corio, S.D.M. Brown, S.A. Empedocles, M.G. Bawendi, G. Dresselhaus, and M.S. Dresselhaus, Braz. J. Phys. **30**, 423 (2000).
[7] C. Thomsen, Phys. Rev. B **61**, 4542 (2000).
[8] S.D.M. Brown, A. Jorio, M.S. Dresselhaus, and G. Dresselhaus, Phys. Rev. B **64**, 073403 (2001).
[9] M.A. Pimenta, A. Jorio, S.D.M. Brown, A.G. Souza Filho, G. Dresselhaus, J.H. Hafner, C.M. Lieber, R. Saito, and M.S. Dresselhaus, Phys. Rev. B **64**, R041401 (2001).
[10] A. Grueneis, M. Hulman, Ch. Kramberger, T. Pichler, K. Peterlik, H. Kuzmany, H. Kataura, and Y. Achiba, in *Proceedings of the International Winter School on Electronic Properties of Novel Materials* (AIP, Woodbury, 2001, in press).
[11] J.H. Hafner, C.L. Cheung, T.H. Oosterkamp, and C.M. Lieber, J. Phys. Chem. B **105**, 743 (2001).
[12] A. Jorio, A.G. Souza Filho, G. Dresselhaus, M.S. Dresselhaus, R. Saito, J.H. Hafner, C.M. Lieber, F.M. Matinaga, M.S.S. Dantas, and M.A. Pimenta, Phys. Rev. B **63**, 245416 (2001); A. Jorio, R. Saito, J.H. Hafner, C.M. Lieber, M. Hunter, T. McClure, G. Dresselhaus, and M.S. Dresselhaus, Phys. Rev. Lett. **86**, 1118 (2001).
[13] M.A. Pimenta, A. Marucci, S.A. Empedocles, M.G. Bawendi, E.B. Hanlon, A.M. Rao, P.C. Eklund, R.E. Smalley, G. Dresselhaus, and M.S. Dresselhaus, Phys. Rev. B **58**, R16 016 (1998).
[14] L. Alvarez, A. Righi, T. Guillard, S. Rols, E. Anglaret, D. Laplaze, and J.L. Sauvajol, Chem. Phys. Lett. **316**, 186 (2000).
[15] P.M. Rafailov, H. Jantoljak, and C. Thomsen, Phys. Rev. B **61**, 16 179 (2000).
[16] A. Jorio, A.G. Souza Filho, G. Dresselhaus, M.S. Dresselhaus, A.K. Swan, M.S. Ünlü, B.B. Goldberg, M.A. Pimenta, J.H. Hafner, C.M. Lieber, and R. Saito, Phys. Rev. B (submitted).
[17] A. Kasuya, Y. Sasaki, Y. Saito, K. Tohji, and Y. Nishina, Phys. Rev. Lett. **78**, 4434 (1997).
[18] A.G. Souza Filho, A. Jorio, A.K. Swan, M.S. Ünlü, B.B. Goldberg, R. Saito, M.A. Pimenta, G. Dresselhaus, and M.S. Dresselhaus, Phys. Rev. B (submitted).
[19] H. Wilhelm, M. Lelausian, E. McRae, and B. Humbert, J. Appl. Phys. **84**, 6552 (1998).
[20] R. Saito, G. Dresselhaus, and M. S. Dresselhaus, *Physical Properties of Carbon Nanotubes* (Imperial College Press, London, 1998).
[21] A.C. Ferrari and J. Robertson, Phys. Rev. B **64**, 075414 (2001).
[22] R. Saito, A. Jorio, A.G. Souza Filho, G. Dresselhaus, M.S. Dresselhaus, and M.A. Pimenta, Phys. Rev. Lett. (accepted).
[23] The joint density of electronic states (JDOS) is given by $\text{JDOS}(\hbar\omega)=(1/4\pi^3)\int\delta[E_i^c(k)-E_i^v(k)-\hbar\omega]dk$, where E_i^c and E_i^v are the energies for the ith electronic state in the conduction (c) and valence (v) bands, respectively.
[24] R. Saito, G. Dresselhaus, and M.S. Dresselhaus, Phys. Rev. B **61**, 2981 (2000).
[25] A.M. Rao, J. Chen, E. Richter, U. Schlecht, P.C. Eklund, R.C. Haddon, U.D. Venkateswaran, Y.K. Kwon, and D. Tománek, Phys. Rev. Lett. **86**, 3895 (2001).
[26] J. Kürti, G. Kresse, and H. Kuzmany, Phys. Rev. B **58**, R8869 (1998).